A Benchmark Airplane Model with Ducts

A. Maicke[1], J. T. Kelley[1], B. MacKie-Mason[2], C. C. Courtney[2], S. Cox[2], D. A. Chamulak[2], G. Burchuk[2], A. E. Yilmaz[2]
(1) University of Texas at Austin, Austin, TX (ajmaicke@utexas.edu)
(2) Lockheed Martin Aeronautics, Palmdale, CA

Abstract—A recently introduced full-size airplane model is upgraded to encourage and support advances in computational electromagnetics. To increase the complexity of scattering problems defined using the model, surfaces covering the intake and exhaust entrances are removed and curved ducts are defined. The ducts are terminated at simple surfaces to reduce requirements on geometric tolerances, support additive manufacturing of scale models, and increase reproducibility of measurements and simulations. To facilitate the benchmarking of as many computational methods as possible, data are shared on a version-controlled online repository to include: (1) exterior surface (outer mold line) of the CAD model, including precise duct definitions, (2) triangular surface meshes of various resolutions, and (3) measured and predicted radar-cross-section data of scale models approximated as perfect electric conductors.

Keywords—computational electromagnetics; benchmarks

I. Introduction

Most case studies in computational electromagnetics (CEM) that analyze scattering from intricate models with complex geometries are not reproducible [1]. This is in part because the few equations, drawings, or figures used in common venues for scientific publications can define only simplistic models accurately. This limitation poses a barrier to the empirical testing and independent corroboration/falsification of the findings of computational scientists and engineers who investigate scattering phenomena using CEM methods. Fortunately, ongoing advances in hardware and software infrastructure make it possible to preserve and share large datasets. Indeed, extremely complex models have been made available online recently [1]–[3]. While it is relatively easy to use these models—e.g., to test the accuracy, quantify the computational costs, and identify the limitations of CEM methods and their software implementations—it is a considerable challenge to develop them.

In [1], the authors developed a high-fidelity full-size re**P**roducible p**RI**ntable electro**M**agn**E**tic (PRIME) airplane model and added it to the Austin RCS Benchmark Suite [4]. Due to the scarcity of precedents for sharing models of such complexity and to increase reproducibility, several key decisions were made during development of the CAD model [1]. In particular, the PRIME model's engine intake and exhaust entrances were covered to avoid open cavities, reducing sensitivity to small perturbations and simplifying cross-validation of simulations and measurements [5]. In this article, building on the work in [1], three entrances to the aircraft model are opened and curved ducts are introduced. The new model is added to the Austin RCS Benchmark Suite as part of the problem set IV-C [6].

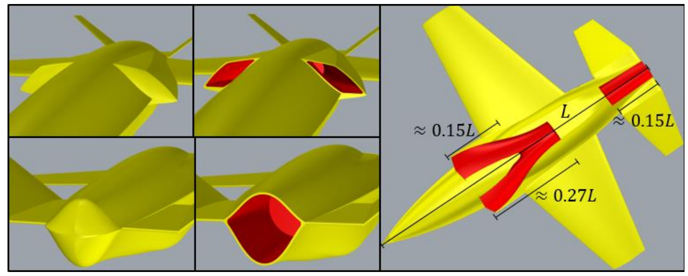

Fig. 1. Visualizations of the PRIME airplane models: Covered vs. open intake (top left). Covered vs. open exhaust (bottom left). Shapes and locations of the ducts inside the fuselage (right).

II. Model Development

A. Building the Open-Duct Model

The development of the airplane model without ducts is described in [1]. That no-duct model is used to define problem sets IV-A (a perfect-electrically-conducting (PEC) model) and IV-B (a homogenous dielectric model) in [4]. The ducts added to the model have precisely-defined curved surfaces that terminate at flat circular surfaces inside the fuselage. The engine intake duct has two separate cavity openings symmetrically placed about the xz plane (see Fig. 2) that are joined inside the fuselage. Opening the exhaust duct reduces the length of the full-sized model from $L \approx 15.1$ m to $L \approx 14.8$ m. Rather than joining them at sharp edges, the ducts were mated with the fuselage using small flange surfaces. Fig. 1 shows the lengths and locations of the ducts in the model.

The ducts were initially defined and joined to the rest of the PRIME model with the same CAD tool used to design the airplane [7]. The resulting model was exported in IGS and STL formats. The STL file was used to 3D print open-duct scaled models that were measured. The IGS file was used to join the ducts with the no-duct model developed in [1]; specifically, the duct surfaces were imported, the duct entrances were removed into the model in [1], and the surfaces were joined to create the new open-duct model. The resulting model was exported as an IGS file to a commonly used software to generate meshes for CEM analysis. Just as in [1], the cavities in the IGS file could not be easily meshed and had to be defeatured. This involved merging small surfaces into their neighbors and aligning surface edges to best allow mesh conforming across surface edges while maintaining the outer mold line (OML) of the airplane to the greatest extent possible. This process reduced the number of surfaces forming the cavities from 52 to 46. Upon removing the exhaust entrance some of the immediately adjacent surfaces near the tail of the IGS model needed to have their edges aligned to accommodate the ducts. Between the addition of the cavities and the edge alignments made near the tail, the number of surfaces

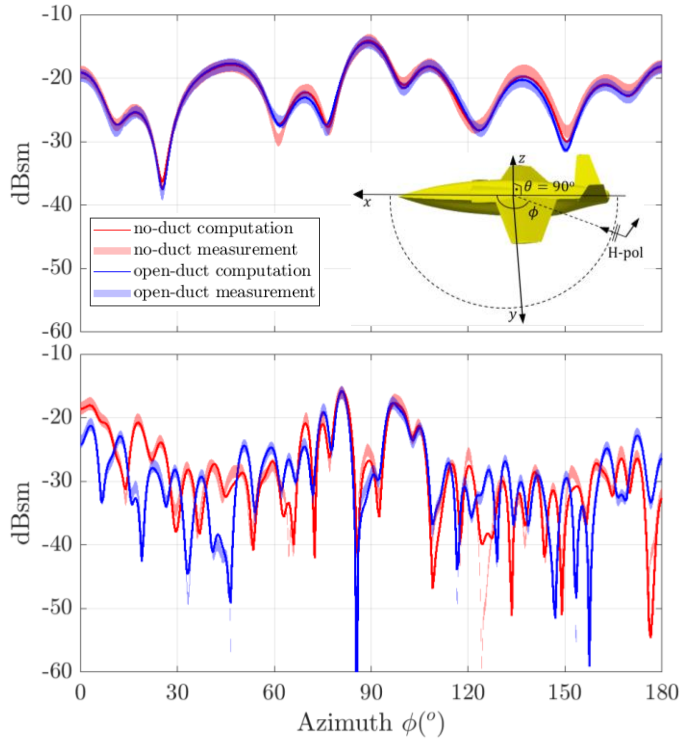

Fig. 2. Simulated and measured RCS data (HH-polarization) for both the no-duct and open-duct scaled PRIME models at (top) 2.56 GHz and (bottom) 10.24 GHz. The shaded regions represent a ±1 dB uncertainty window surrounding the measured data.

increased from 108 to 166 for the open-duct PRIME model. As with the no-duct model, it is possible to mesh only half of these surfaces and reflect across the xz plane, leaving only 83 unique surfaces to mesh. To simplify the use of the model, a series of triangular meshes of varying resolution was generated and also provided in two different file formats in [6].

B. Electromagnetic Evaluation

The open-duct PEC PRIME model's monostatic radar-cross-section (RCS) was measured and computed for a scaled $L \approx 9$ in model. Results at 2.56 GHz (pre-cutoff for all modes in the waveguides formed in the ducts) and 10.24 GHz (post-cutoff) are compared to those for the no-duct PRIME model in Fig. 2. The simulated data was calculated using the ARCHIE-AIM, a code developed at the University of Texas at Austin [8]. The simulations were performed by discretizing the model's surface with triangular elements. Fig. 2 shows that the results for the open- and no-duct models are quite similar at 2.56 GHz as should be expected when fields in the ducts are cutoff. At the higher frequency, cavity scattering effects are prominent and the results for the open-duct model differ significantly from the no-duct model for the look angles $0° \leq \phi \leq 75°$ (looking toward the intake) and $120° \leq \phi \leq 180°$ (looking toward the exhaust). As a second validation, simulation results are compared to measurement data in Fig. 2. Remarkable agreement is observed between measurements and simulations for both the no-duct and the open-duct models at both frequencies. These data were measured at Lockheed Martin Aeronautics' Rye Canyon facility [8],[9] using additively manufactured scaled models (Fig. 3).

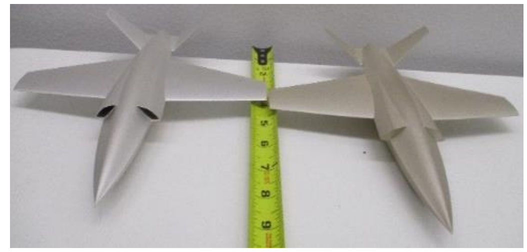

Fig. 3. Two additively manufactured scaled models ($L \approx 9$ in). The open-duct (left) PRIME model is about 2% shorter than the no-duct (right) version.

The IGS and STL files defining the airplane's OML as well as mesh files for the open-duct model are available at [6]. Additionally, simulated and measured RCS data for the open-duct model are also made available in [6] as part of problem set IV-C.

III. Conclusion

The PRIME airplane model has been upgraded by removing the engine intake and exhaust coverings and revealing ducts behind them. The new model supports more complicated scattering phenomena due to presence of open cavities [5]. To encourage its use for benchmarking modern CEM methods, the open-duct PRIME airplane model is used to define problem set IV-C in the Austin RCS Benchmark Suite.

Acknowledgment

The authors acknowledge the Texas Advanced Computing Center (TACC) at The University of Texas at Austin for providing HPC resources that have contributed to the research results reported in this article.

References

[1] J. T. Kelley, A. Maicke, D. A. Chamulak, C. C. Courtney, and A. E. Yilmaz, "Adding a reproducible airplane model to the Austin RCS benchmark suite," in *Proc. Appl. Comp. Electrom.. Soc. Symp.*, July 2020.

[2] J. W. Massey and A. E. Yilmaz, "AustinMan and AustinWoman: High-fidelity anatomical voxel models developed from the VHP color images," in *Proc. IEEE Eng. Medic. Biology Soc.*, pp 3346–3349, Aug. 2016.

[3] F. Guo *et al.*, "The IEEE EPS packaging benchmark suite," in Proc. *IEEE Elect. Perform. Electron. Packag. Syst. (EPEPS)*, Oct. 2021.

[4] J. W. Massey, J. T. Kelley, C. Courtney, D. A. Chamulak, and A. E. Yilmaz, "A benchmark suite for quantifying RCS simulation performance on modern computers," in *Proc. USNC/URSI Rad. Sci. Meet.*, July 2018.

[5] A. E. Yilmaz *et al.*, "Camera boxes: A set of complex scattering problems to test EM measurements and simulations," in *Proc. IEEE Ant. Prop. Soc. Int. Symp.*, 2022.

[6] "Austin Benchmark Suites for Computational Electromagnetics", 2018. [Online]. Available: https://github.com/UTAustinCEMGroup/AustinCEMBenchmarks

[7] C. Davies, "Lockheed Martin overview of the AFRL EXPEDITE program," *Proc. AIAA Scietech*, pp. 1-12, Jan. 2019.

[8] J. T. Kelley, D. A. Chamulak, C. C. Courtney, and A. E. Yilmaz, "Rye Canyon RCS measurements of benchmark almond targets," *IEEE. Ant. Prop. Soc. Mag.*, vol. 62, no. 1, pp. 96–106, Feb. 2020.

[9] J. T. Kelley, D. A. Chamulak, C. C. Courtney, and A. E Yilmaz, "Measurements of non-metallic targets for the Austin RCS Benchmark Suite," in *Proc. Ant. Meas. Tech. Assoc.*, Oct. 2019.